Depolarized light scattering from critical polymer blends

*Alexander N. Semenov**[1], *Alexei E. Likhtman*[1,2], *Dimitris Vlassopoulos*[3], *Kostas Karatasos*[3,4], *George Fytas*[3,5]

[1] Department of Applied Mathematics, University of Leeds, Leeds LS2 9JT, U.K.
[2] Moscow State University, Physics Department, Moscow 117234, Russia
[3] FORTH, Institute of Electronic Structure and Laser, P.O. Box 1527, 71110 Heraklion, Crete, Greece
[4] Department of Physics and Astronomy, University of Leeds, Leeds LS2 9JT, U.K.
[5] Max Plank Institute for Polymer Research, P.O. Box 3148, 55021 Mainz, Germany

(Received: September 28, 1998; revised: November 16, 1998)

SUMMARY: Depolarized light scattering of binary polymer blends in disordered state near the demixing critical point is considered both theoretically and experimentally. It is shown that the depolarized scattering in such systems is predominantly due to double scattering processes induced by composition fluctuations. For long enough polymer chains, this scattering is stronger than the contribution from intrinsic anisotropy fluctuations. The general equation for the static and dynamic double scattering function is obtained in terms of the system structure factor. The scattering functions are calculated both analytically and numerically (dynamic part) for polymer blends. We found that the depolarized intensity depends on the polymerization degree N and the relative distance from the critical point $\tau = 1 - \chi^*/\chi$ (where χ is the Flory-Huggins interaction parameter and χ^* its critical value) as $I_{vh} \sim N^2/\tau^2$, which is in good agreement with the experimental data. It is also shown that the dynamic scattering function is decaying non-exponentially. We calculate the relaxation rate and the non-exponentiality parameter as functions of the scattering angle and τ. These theoretical predictions are compared with experimental data for three chemically different blends.

1. Introduction

Polymer blends often phase separate in a certain temperature range[1)]. Their critical behavior near the boundary of this range has received much attention recently[2)]. The aim of the present paper is to consider both theoretically and experimentally the depolarized light scattering from composition fluctuations in a disordered (i.e. not yet phase separated, macroscopically uniform) blend near its critical point[3)].

Let us consider a typical light scattering set up when a vertically polarized initial beam is scattered in the horizontal plane. The vertical component of the scattered light is then usually denoted as VV, and the horizontal one as VH. The theory of single VV scattering from composition fluctuations is well known[2,4–7)].

The scattering intensity is proportional to the correlation function of the dielectric polarizability:

$$I_{vv}^{(1)}(q) = \frac{cR_0^2}{8\pi}\langle E_{vv}E_{vv}^*\rangle = I_0 k_0^4 \langle \delta æ(\mathbf{q})\delta æ(-\mathbf{q})\rangle \qquad (1)$$

where k_0 and k are the wavevector of the incident and the scattered light, respectively, c is the light speed in vacuum, $\mathbf{q} = \mathbf{k} - \mathbf{k}_0$ is the scattering vector, R_0 is the distance from the scattering sample to the detector, $I_0 = \frac{cE_0^2}{8\pi}$ is the intensity of the initial beam, E_0 is the electric field amplitude of the initial beam, and $\delta æ(q) = \int \delta æ(r) \exp(\mathrm{i}qr)\mathrm{d}^3r$ is the dielectric polarizability fluctuation in the Fourier representation. Note that we define the scattered intensity as the energy scattered into a unit spatial angle per unit time.

For a blend of A and B homopolymers, the scattering intensity can be further related to the structure factor of composition fluctuations[a]:

$$\delta æ(r) = \frac{A}{2\pi}\delta\phi(r) \qquad \delta\phi(r) = \phi(r) - \langle\phi(r)\rangle \qquad (2)$$

where $\phi(r) \equiv \phi_A(r)$ is the local volume composition of A monomers, $A = \frac{\partial n}{\partial \phi}$ is the refractive index contrast ($n = n(\phi)$), and we assume as usually local incompressibility of the blend $\phi_A(r) + \phi_B(r) = 1$ for any $\mathbf{r}$. Using eqs. (1) and (2) we get

$$I_{vv}^{(1)}(q) = I_0 k_0^4 \left(\frac{A}{2\pi}\right)^2 S(q) \qquad (3)$$

where $S(q) = \int \langle \delta\phi(r)\delta\phi(0)\rangle \exp(\mathrm{i}qr)\mathrm{d}^3r$ is the structure factor.

For a symmetric blend with number of monomers per chain $N_A = N_B = N$ and statistical segment length $\sqrt{6}a$ ($a_A = a_B = a$ and mean square end-to-end distance is $\langle R^2\rangle = 6Na^2$) the mean field structure factor is[1)]

[a] Both fluctuations of total density and composition fluctuations contribute to the scattering intensity in the general case. However the density contribution is normally negligible for polymer blends[6)].

  1022-1344/99/0305–0179$17.50+.50/0

$$S^{-1}(\mathbf{q}) = \frac{1}{\phi N g(Na^2q^2)} + \frac{1}{(1-\phi)Ng(Na^2q^2)} - 2\chi$$

where χ is the Flory-Huggins parameter, $\phi = \langle\phi_A\rangle$ is the average composition, and

$$g(x) = \frac{2}{x^2}(x + e^{-x} - 1)$$

is the Debye function.

Near the critical point ($\phi^* = 0.5$, $\chi^* N = 2$) the structure factor can be approximated as

$$S(\mathbf{q}) = \frac{S(0)}{1 + \xi^2 q^2} \tag{4}$$

where $S(0) = \frac{Nv}{4\tau}$, $\xi = R/\sqrt{18\tau}$ is the correlation length of the composition fluctuation, $\tau = (1 - \chi/\chi^*)$ is the relative distance to the critical point, and v, the monomer volume. Substituting eq. (4) into eq. (3) we get for the single scattering intensity,

$$I_{vv}^{(1)} = I_0 k_0^4 \left(\frac{A}{2\pi}\right)^2 \frac{Nv}{4\tau} \frac{1}{1 + \xi^2 q^2} \tag{5}$$

which is proportional to N/τ.

It is well known that single scattering from composition fluctuations does not produce a depolarized component[4]: $I_{vh}^{(1)} \equiv 0$. On the other hand it is known that multiple scattering does give rise to non-zero depolarized intensity[8]. In the present paper, we show that the dominant contribution to the depolarized intensity arises from double scattering (schematically depicted in Fig. 1) characterized by a qualitatively different temperature dependence compared to the polarized scattering $I_{vv}^{(1)}$.

The paper is organized as follows. In section 2 we consider the double scattering process qualitatively and show that it produces a dominant contribution to the depolarized intensity as compared to the scattering from orientational fluctuations. A quantitative description of the average double scattering intensity and the corresponding intermediate (dynamic) scattering function are considered respectively in sections 3 and 4. Section 5 is devoted to calculation of the static intensity for a realistic experimental setup, whereas in the Appendix B we formulate the renormalization procedure establishing the scattering properties of the system with arbitrary refractive index. The theoretical (static and dynamic) results and experimental data are compared in section 6 and the concluding remarks can be found in the last section 7. Appendix A is dedicated to the derivation of main theoretical results for the depolarized intensity of a double scattering wave.

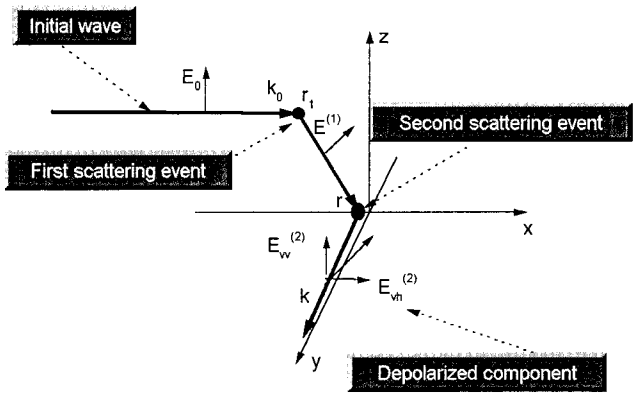

Fig. 1. Schematic illustration of the double scattering process

2. Scaling results

We consider possible mechanisms for depolarized (VH) scattering for homogeneous polymer blends near their critical point. Like in amorphous homopolymers, one source of depolarized scattering is orientational fluctuations of polymer segments[5, 9, 10]:

$$I_{vh}^{ani} \sim I_0 k_0^4 \beta_s^2 / v \tag{6}$$

where β_s is the segmental optical anisotropy. Obviously this intensity does not depend on N (and so the scattering on anisotropy fluctuations is not a polymer-specific effect) and we will show below that it is negligible for sufficiently long chains.

Another source of depolarized scattering is multiple scattering from composition fluctuations. Since normally the higher the scattering order, the smaller the scattering amplitude, we expect that it is the *double* scattering from composition fluctuations that might provide the dominant contribution to the VH intensity. For an estimation of the latter (omitting numerical factors) we consider first single scattering of a finite volume $V \sim L^3$ of typical size L. The scattered intensity (per unit scattering volume) is given by eq. (3). Let E_1 be the amplitude of the scattered field inside the volume, the total scattered intensity $VI_1 \sim VI_0 k_0^4 A^2 S(q)$ must be roughly equal to $cE_1^2 L^2$, where L^2 is about the surface area of the scattering volume. Thus, $E_1^2 \sim E_0^2 L k_0^4 A^2 S(q)$. Now we apply eq. (3) again in order to get the intensity of the double scattered wave:

$$I_{vh}^{(2)} \sim E_1^2 k_0^4 A^2 S(q)$$

If $q\xi \ll 1$ and $q \sim k_0$, then we can use the mean-field result of eq. (4) for a symmetric near critical blend: $S(q) \approx S(0) \sim Nv/\tau$. So the scaling result for the VH intensity is

$$I_{vh}^{(2)} \sim I_0 A^4 k_0^8 L S^2(k_0) = I_0 A^4 k_0^8 L N^2 v^2 / \tau^2$$

Thus, we predict stronger N and τ dependencies of I_{vh} compared to the polarized intensity, $I_{vv} \propto S(0)$. It is the

strong molecular weight dependence of I_{vh} that makes the VH scattering of composition fluctuations a polymer-specific effect.

The ratio of the scattering intensity due to anisotropy fluctuations and double scattering is

$$\frac{I_{vh}^{ani}}{I_{vh}^{(2)}} \sim \frac{\beta_s^2 \tau^2}{N^2 v^3 k_0^4 L A^4}$$

This ratio is of order of 10^{-2} for polystyrene (PS)/poly(isoprene) (PI) and PS/polybutadiene (PB) blends[3]; for the poly(dimethylsiloxane) (PDMS)/poly(ethylmethylsiloxane) (PEMS) system[3] the segmental β_s is negligibly low. Thus double scattering of composition fluctuations should dominate in the VH intensity for all blends.

3. Analytical theory

We consider the initial beam with polarization vector $\mathbf{e}_0$ parallel to z axis and wave vector $\mathbf{k}_0$ parallel to x axis: $\mathbf{E}^{(0)} = \mathbf{e}_0 E_0 e^{i(\mathbf{k}_0 \mathbf{r} - \omega t)}$. First we consider the case of finite scattering sample, a sphere of radius L, so that the scattering volume is $V = 4\pi L^3/3$, and the size of the sample is larger than the wavelength of scattered light: $Lk_0 \gg 1$. The initial beam is assumed to be a plane wave of infinite width (this approximation is lifted below, see section 5).

The electric field induces dipole polarization in the scattering volume: $\mathbf{d}(\mathbf{r}, t) = æ(\mathbf{r})\mathbf{E}^{(0)}(\mathbf{r}, t)$, where $æ(\mathbf{r})$ is the polarizability of the medium at point $\mathbf{r}$. The corresponding single scattered wave is[11]:

$$\mathbf{E}^{(1)}(\mathbf{r}, t) = \int \left\{ \text{grad div} \frac{\mathbf{d}(\mathbf{r}_1, t - \frac{|\mathbf{r}_1 - \mathbf{r}|}{c})}{|\mathbf{r}_1 - \mathbf{r}|} + \left(\frac{\omega}{c}\right)^2 \frac{\mathbf{d}(\mathbf{r}_1, t - \frac{|\mathbf{r}_1 - \mathbf{r}|}{c})}{|\mathbf{r}_1 - \mathbf{r}|} \right\} d^3\mathbf{r}_1 \qquad (7)$$

The intensity of the single scattered wave at large distance R_0 ($R_0 \gg L$) from the scattering volume is $I = \frac{cR^2}{8\pi} \langle (\mathbf{E}\mathbf{e}_1)(\mathbf{E}^*\mathbf{e}_1) \rangle$, where $\mathbf{e}_1$ is the unit vector defining the polarization of the scattered wave

$$I^{(1)} = (\mathbf{e}_0\mathbf{e}_1)^2 I_0 k_0^4 \int \langle æ(0) æ(r_1) \rangle e^{i(\mathbf{k}-\mathbf{k}_0)\mathbf{r}_1} d^3 r_1$$

$$= (\mathbf{e}_0\mathbf{e}_1)^2 I_0 k_0^4 \frac{A^2}{(2\pi)^2} S(q)$$

where $\mathbf{q} = \mathbf{k} - \mathbf{k}_0$, and $\mathbf{k}$ is the wave vector of the scattered wave. In the case of VV scattering ($\mathbf{e}_1$ parallel to $\mathbf{e}_0$) we get eq. (3) and the intensity is zero for $\mathbf{e}_1$ parallel to the x-y plane (VH scattering): $I_{vh}^{(1)} = 0$.

For a double scattering process, we consider a dipole moment at point $\mathbf{r}$, induced by the partial wave $E^{(1)}(\mathbf{r})$ which was produced as a result of single scattering at point $\mathbf{r}_1$ (see Fig. 1). This dipole emits a double scattered wave, its amplitude $E^{(2)}$ is related to $E^{(1)}$ via an equation analogous to eq. (7). The total amplitude of the double scattered wave is given by the double integral $d^3r_1 d^3r$ over all possible pairs of scattering points r_1 and r:

$$\mathbf{E}_{vh} = k_0^2 \frac{e^{i\frac{\omega}{c}R_0}}{R_0} \int æ(\mathbf{r}) e^{-i\mathbf{k}\mathbf{r}} \mathbf{e}_1 \mathbf{E}_1^{(1)}(\mathbf{r}) d^3 r \qquad (8)$$

where $E^{(1)}(r)$ is defined in eq. (7). As we noted before, we are considering a finite scattering sample in this section. Let us define the form factor of the sample $H(\mathbf{r})$ as: $H(\mathbf{r}) = 1$ inside the sample, and $H(\mathbf{r}) = 0$ otherwise. Using the Fourier transformation $H(\mathbf{q}) = \int H(\mathbf{r}) e^{i\mathbf{q}\mathbf{r}} d^3 r$ after some algebra (see Appendix A) we obtain the general equation for the total double scattering intensity:

$$I_{vh} = I_0 k_0^4 \left(\frac{A}{2\pi}\right)^4 \int S(\mathbf{k} - \mathbf{q}) S(\mathbf{q} - \mathbf{k}_0) (f^*(\mathbf{q}) + f^*(\mathbf{k} + \mathbf{k}_0 - \mathbf{q})) \times \left[\int H^2(\mathbf{Q}) f(\mathbf{q} - \mathbf{Q}) \frac{d^3\mathbf{Q}}{(2\pi)^3} \right] \frac{d^3\mathbf{q}}{(2\pi)^3} \qquad (9)$$

where

$$f(\mathbf{q}) = 4\pi \frac{(\mathbf{e}_0\mathbf{q})(\mathbf{e}_1\mathbf{q})}{\mathbf{q}^2 - (k_0 + i0)^2}$$

$i = \sqrt{-1}$ and 0 denotes an infinitesimal positive number.

The function $f(\mathbf{q})$ is singular near the sphere $|\mathbf{q}| = k_0$ in the wave-vector space. Therefore it is the vicinity of this sphere that gives dominant contribution to I_{vh} in the limit $L \to \infty$, i.e. when Q is sufficiently small: $Q \sim 1/L \to 0$. In order to simplify the calculation of this integral let us approximate the form factor by a Gaussian function: $H(\mathbf{r}) = e^{-\frac{\beta r^2}{L^2}}$, $H(\mathbf{q}) = L^3(\pi/\beta)^{3/2} e^{-\frac{L^2 q^2}{4\beta}}$ where the coefficient $\beta = 3^{2/3}\pi^{1/3}2^{-7/3}$ is defined by the condition $\int H^2(\mathbf{r}) d^3 r = V = 4\pi L^3/3$.

After substitution of $H(\mathbf{q})$ and $S(\mathbf{q})$ (eq. (4)), the integral of eq. (9) for large but finite L ($Lk_0 \gg 1$) is dominated by two regions: the spherical zone $|q - k_0| \lesssim 1/L$ and the region $q \sim 1/\xi \gg k_0$. We consider the corresponding singular and non-singular parts separately.

The singular part can be calculated analytically in the limit $k_0 L \gg 1$.

The result for singular VH intensity I_{vh}^s is:

$$I_{vh}^s = I_0 \frac{A^4 V}{(2\pi)^4} k_0^8 S^2(0) L \frac{\pi^{4/3} 2^{8/3}}{5 \times 3^{4/3}} \Omega(\theta, k\xi) \qquad (10)$$

$$\Omega(\theta, k\xi) = \frac{15}{4\pi} \cdot \iint \frac{\sin^3\theta_q \cos^2\theta_q \sin^2(\varphi_q - \theta) d\varphi_q d\theta_q}{(1 + 2k^2\xi^2(1 - \sin\theta_q \cos(\varphi_q - \theta)))(1 + 2k^2\xi^2(1 - \sin\theta_q \cos\varphi_q))}$$

where θ is the scattering angle. Note that $\Omega(\theta, k\xi) \to 1$ in the limit $k_0\xi \ll 1$. Expanding Ω $(\theta, k\xi)$ in Taylor series for small $k\xi$ we get

$$\Omega(\theta, k\xi) = 1 - 4(k\xi)^2 + \frac{(k\xi)^4}{7}(100 + 4\cos\theta - 8\cos^2\theta) + O((k\xi)^6)$$

Hence the I^s_{vh} intensity attains a maximum at θ = arccos $\frac{1}{4} \approx 75.5^\circ$.

The nonsingular part can be also calculated analytically in the limit $k_0\xi \ll 1$. The result is

$$I^{ns}_{vh} = I_0 \frac{A^4 V}{(2\pi)^4} k_0^4 S^2(0) \frac{1}{\xi^3} \frac{4\pi}{15} \tag{11}$$

The ratio of singular to nonsingular contributions is

$$\frac{I^s_{vh}}{I^{ns}_{vh}} = L k_0^4 \xi^3 \left(\frac{4\pi}{3}\right)^{1/3} \tag{12}$$

Clearly the non-singular part is negligible if $k_0\xi \sim 1$, or $k_0\xi \gg 1$ since $Lk_0 \gg 1$, so we do not need to consider non-singular contributions in these regimes. Hence, only in the regime $k_0\xi \ll 1$ where eq. (11) is valid, far above the critical point (i.e., where ξ is small), the non-singular contribution can compete with the singular one.

4. Dynamic depolarized scattering

The scattered field time correlation function $I(t) = \frac{cR_0^2}{8\pi} \langle E(0)E^*(t)\rangle$ (see eq. (1)) can be obtained from photon correlation spectroscopy measurements. It is easy to show that eqs. (3) and (9) can be generalized for the dynamic case as follows:

$$I^{(1)}_{vv}(t) = I_0 k_0^4 \frac{A^2}{(2\pi)^2} S(\mathbf{k} - \mathbf{k}_0, t) \tag{13}$$

$$I_{vh}(t) = I_0 k_0^4 \left(\frac{A}{2\pi}\right)^4 \int S(\mathbf{k} - \mathbf{q}, t) S(\mathbf{q} - \mathbf{k}_0, t)(f^*(\mathbf{q}) + f^*(\mathbf{k} + \mathbf{k}_0 - \mathbf{q})) \left[\int H^2(\mathbf{Q}) f(\mathbf{q} - \mathbf{Q}) \frac{\mathrm{d}^3 Q}{(2\pi)^3}\right] \frac{\mathrm{d}^3\mathbf{q}}{(2\pi)^3} \tag{14}$$

where $S(\mathbf{q}, t) = \int \langle \phi(\mathbf{r}, t)\phi(0,0)\rangle \, \mathrm{e}^{i\mathbf{qr}} \mathrm{d}^3 r$ is the dynamic structure factor (the intermediate scattering function); we assume that $qt \gg c^{-1}$, where t is the shortest relaxation time that we consider.

Near the critical point the dynamic structure factor can be approximated as $S(\mathbf{q}, t) \approx S(\mathbf{q}, 0)\mathrm{e}^{-Dq^2 t}$, where D is the cooperative diffusion constant. Using eqs. (13) and (14) we obtain the corresponding intermediate scattering functions for the single polarized and double depolarized (singular contribution, $k\xi \ll 1$) scattering components:

$$I_{vv}(\mathbf{q}, t) = I_{vv}(\mathbf{q}, 0)\mathrm{e}^{-\Gamma_0 \sin^2(\theta/2)\mathrm{t}} \tag{15}$$

$$I^s_{vh}(\mathbf{q}, t) = I^s_{vh}(\mathbf{q}, 0)\mathrm{e}^{-\Gamma_0 t}(\cos^2(\theta/2)\Xi_1(\Gamma_0 \cos(\theta/2)t) + \sin^2(\theta/2)\Xi_2(\Gamma_0 \cos(\theta/2)t)) \tag{16}$$

where $\Gamma_0 = 4Dk_0^2$ and

$$\Xi_1(a) = \frac{15}{a^5}(a^2 \sinh a - 3a\cosh a + 3\sinh a)$$

$$\Xi_2(a) = \frac{15}{a^5}(a^3 \cosh a - 5a^2 \sinh a + 12a\cosh a - 12\sinh a)$$

Thus, in contrast to the simple exponential decay of the dynamic VV scattering function, we predict a non-exponential decay for the VH process, in agreement with the experimental data (see section 6).

For $k_0\xi \approx 1$ the dynamic scattering functions are calculated using numerical integration. The relaxation function $I^s_{vh}(\mathbf{q}, t)$ is approximated by a stretched exponential function $\exp(-(\Gamma t)^\beta)$, where Γ is the relaxation rate and β (≤ 1) is the non-exponentiality parameter. The theoretical angular dependencies of these fitting parameters for different $k_0\xi$ are shown in Fig. 2. The case $k_0\xi$ = 0 corresponds to eq. (16) the solid line corresponds to the VV single scattering (eq. (15)).

We see that the VH relaxation rate is predicted to be equal to the VV relaxation rate for θ =180°: $\Gamma_{VH} = \Gamma_{VV} = 4Dk_0^2$. Both VV and VH relaxations slow down when θ decreases towards θ = 0. However the decrease of purely diffusive Γ_{VV} is more pronounced: Γ_{VV} = 0 for θ = 0, whereas Γ_{VH} decreases down to a constant rate. The decrease of Γ_{VH} is more steep near the critical point (for small τ, i.e. large $k_0\xi$) and becomes weaker with increasing distance from the critical temperature (low $k_0\xi$). Note that as for the VH process the dynamic scattering function has non-exponential form, eq. (16), so that the relaxation rate depends on the time range where we approximate it by a stretched exponential function. At short t the VH correlation function eq. (16) decreases with constant rate $\Gamma^{(0)}_{vh} = 4Dk_0^2$, but for large t the rate is slower: $\Gamma^{(\infty)}_{vh}$ = (1 – cos $\frac{\theta}{2}$)$4Dk_0^2$. This range of large t is responsible for the decrease of Γ_{vh} with decreasing θ; its contribution increases with increasing $k_0\xi$. For θ = 180° both relaxation times are equal, and for $\theta \to 0$ the scattering function decays according to a power law at long times, i.e., $\Gamma^{(\infty)}_{vh}$ = 0. We thus predict a spectrum of processes with relaxation rates ranging from $\Gamma^{(\infty)}_{vh}$ to about $\Gamma^{(0)}_{vh}$. Note that scattering experiments at θ = 180° are impossible.

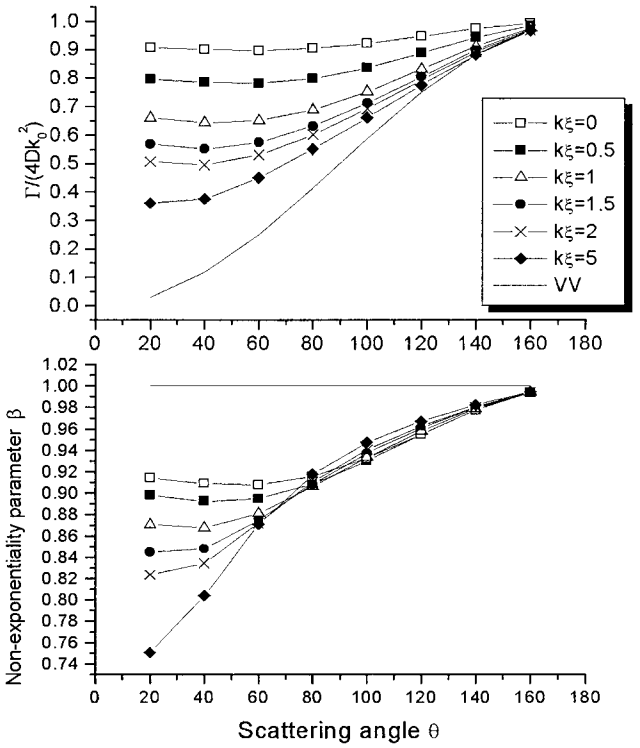

Fig. 2. Theoretical predictions for the angular dependence of the normalized ($\Gamma/(4Dk_0^2)$) relaxation rate Γ and of the non-exponentiality parameter β for the scattering function (eqs. (15), (16)). Lines with symbols correspond to VH scattering, lines without symbols correspond to VV scattering

The non-singular contribution to the dynamic structure factor of eq. (14) (region of large **q**) is:

$$I_{vh}^{ns}(t) = I_{vh}^{ns}(0) J\left(\frac{Dt}{\xi^2}\right)$$

where

$$J(a) = \frac{2}{\pi}\int_0^\infty \frac{\mathrm{e}^{-ay}\sqrt{y}}{(1+y)^2}\mathrm{d}y = \begin{cases} 1-4\sqrt{a/\pi}, & a \ll 1 \\ \frac{1}{\sqrt{\pi a^{3/2}}}, & a \gg 1 \end{cases}$$

Thus the relation rate corresponding to this term is $\Gamma_{ns} \sim D/\xi^2$, i.e., Γ_{vh}^{ns} is higher than the singular relaxation rate if $k_0\xi$ is small. However, as we show, the non-singular contribution is small for the systems under consideration (see section 6).

5. Finite width effects

Let us consider now a different setup. We assume that the scattering sample is infinite, but the width of the initial and scattered beams is finite with characteristic radii L_i and L_p respectively. This situation is close to the real experimental setup, where L_p was a radius of pinholes for the outcoming beam (see section 6) with L_i = 0.5 mm and L_p = 0.1 mm[3,7].

The initial beam (along the *x*-axis) is characterized by

$$\mathbf{E}^{(0)} = \mathbf{e}_0 B(y,z) E_0 \mathrm{e}^{\mathrm{i}(\mathbf{k}_0\mathbf{r}-\omega t)} \tag{17}$$

where $\mathbf{k}_0$ is parallel to the *x* axis, E_0 is the electric field amplitude in the center of the beam and the function

$$B(y,z) = \mathrm{e}^{-\frac{\ln 2(y^2+z^2)}{2L_i^2}}$$

describes the dependence of the amplitude on the distance from the beam axis. The definition of L_i implies that the intensity at the distance L_i from the beam axis is 1/2 of the maximum intensity at the beam axis, $I(0)$: $I(L_i) = \frac{1}{2}I(0)$.

Using equation (7) twice (and also using the wave-zone assumption, $|\mathbf{r}-\mathbf{r}_1| \gg 1/k_0$), we can calculate the amplitude of the double scattered VH wave (here all calculations are performed in the real space rather than in the Fourier representation):

$$E_{vh}^s = k_0^4 \iint \text{æ}(\mathbf{r})\,\text{æ}(\mathbf{r_1}) \cdot \frac{(\mathbf{E}^{(0)}(\mathbf{r}_1)(\mathbf{r}-\mathbf{r}_1))((\mathbf{r}-\mathbf{r}_1)\mathbf{e}_1)}{|\mathbf{r}-\mathbf{r}_1|^3} \mathrm{e}^{\mathrm{i}(\mathbf{k}_0\mathbf{r}_1 + k|\mathbf{r}-\mathbf{r}_1|)} \mathrm{d}^3r\,\mathrm{d}^3r_1 \tag{18}$$

Using expression (17) for $\mathbf{E}^{(0)}(\mathbf{r})$, replacing $S(k-k_0)$ by $S(0)$ and assuming that $L_i \gg 1/k_0 \gg \xi$, we get the singular part of the VH intensity:

$$I_{vh}^s = I_0 k_0^8 S^2(0) \int \mathrm{d}^3r_1 \int_{pinholes} \mathrm{d}^3r\, B^2(\mathbf{r}_1) \cdot \left(\frac{(\mathbf{e}_0(\mathbf{r}-\mathbf{r}_1))(\mathbf{e}_1(\mathbf{r}-\mathbf{r}_1))}{|\mathbf{r}-\mathbf{r}_1|^3}\right)^2 \tag{19}$$

where $\mathbf{e}_1$ is the polarization vector of the scattered wave. Here the first integral over $\mathbf{r}_1$ (the point of the first scattering event) should be calculated with infinite limits, and the integral $\int_{pinholes} \mathrm{d}^3r$ is calculated with infinite limits in the *y*-direction and is limited by pinholes in the (*xz*) plane. We have calculated these integrals analytically for the scattering angle $\theta = 90^\circ$. The result is

$$I_{vh}^s = I_0 S^2(0) k_0^8 \left(\frac{A}{2\pi}\right)^4 \frac{\pi^3 L_i^2 L_p^2}{4\ln 2} \tag{20}$$

Note that this result is in agreement with eq. (10), if we take into account that the effective scattering volume is $V_{eff} \sim L_i L_p^2$.

We can use the previous result, eq. (11), in order to calculate the nonsingular term. The total intensity I_{vh}^{ns} is defined by the r.h.s. of eq. (11) multiplied by the scattering volume $V_{eff} = \int_{pinholes} B^2(\mathbf{r})\mathrm{d}^3r$: the nonsingular intensity is a sum of additive local contributions since the relevant wave-vectors q (see eq. (9)) are large, $q \sim 1/\xi \gg$

$1/L_p$. The integral, $\int_{pinholes}$, has the same meaning as in eq. (19):

$$V_{eff} = \int_{-\infty}^{\infty} \mathrm{d}y \int_0^{L_p} r\mathrm{d}r \int_0^{2\pi} \mathrm{d}\varphi \mathrm{e}^{-\frac{\ln 2(y^2+r^2\cos^2\varphi)}{L_i^2}}$$

$$= \frac{L_i^3\sqrt{\pi}}{2\ln^{3/2}2} Q\left(\ln 2 \frac{L_p^2}{L_i^2}\right) \qquad (21)$$

where

$$Q(x) = \int_0^{2\pi} \frac{(1-\mathrm{e}^{-x\cos^2\varphi})}{\cos^2\varphi} \mathrm{d}\varphi \qquad (22)$$

$Q(x) \to 2\pi x$ for $x \ll 1$. In the experiments this parameter is indeed small, $x = \ln 2 \frac{L_p^2}{L_i^2} \approx 0.03$, so we can safely use the $x \ll 1$ asymptotics, and so

$$V_{eff} = \frac{\pi^{3/2}}{\sqrt{\ln 2}} L_i L_p^2$$

The final result for the nonsingular part is

$$I_{vh}^{ns} = I_0 k_0^4 S^2(0) \left(\frac{A}{2\pi}\right)^4 \frac{L_i L_p^2}{\xi^3} \frac{4\pi^{5/2}}{15\sqrt{\ln 2}} \qquad (23)$$

The ratio of the singular to nonsingular parts is

$$\frac{I_{vh}^{s}}{I_{vh}^{ns}} = L_i k^4 \xi^3 \frac{15}{16} \sqrt{\frac{\pi}{\ln 2}}$$

This equation agrees well with eq. (12), except a slight difference in the numerical coefficient (4 instead of 3.22) if we substitute L in eq. (12) by the radius of the initial beam, L_i. It is also useful to note that in the opposite case, $L_p \gg L_i$ $Q(x) \to 6.67\sqrt{x}$, and the nonsingular term is proportional to $L_i^2 L_p$, so that $\frac{I_{vh}^{s}}{I_{vh}^{ns}}$ is proportional to L_p in this regime.

6. Comparison with the experimental data

The experimental setup is characterized by the following parameters: laser wavelength λ = 532 nm, the radius of the initial beam is L_i = 0.5 mm, the radius of pinholes L_p = 0.1 mm. The experimental procedure for the photon correlation spectroscopy (PCS) measurements and the precautions for correct polarization conditions were described in ref.[3] Dilute latex sphere dispersions displaying diffusion dynamics with a polarized (VV) intensity up to 5 Mhz exhibit no dynamic anisotropic scattering over the examined q-range (scattering angle 12 ÷ 150°). In particular, the model PDMS/PEMS blends with very low refractive index contrast (see Tab. 1) have allowed VH measurements very near to T^* and for scattering angles as low as 10°. At these extreme conditions, the polarized intensity reaches the limit imposed by the extinction coefficient ($\sim 10^{-7}$) of the Glan-Thompson analyzer.

Fig. 3 shows the relaxation functions $I_{vv}(q,t)$ and $I_{vh}(q,t)$ for PDMS/PEMS A at T = 40.7°C and θ =12° (q = 3.4×10^{-3} nm^{-1}) obtained from the experimental polarized (VV) and depolarized (VH) intensity autocorrelation functions $G(q,t) \equiv \langle I(q,t)I(q,0)\rangle$; $|C(q,t)| = ((G(q,t) - 1)/f^*)^{1/2}$, where f^* is a known instrumental (coherence) factor. At this low scattering angle, the anisotropic relaxation function is much faster (about 30 times) than the isotropic interdiffusion process. Alternatively, the slow process, with dynamics very similar to the interdiffusion isotropic process (Fig. 3), could partially result from VV leakage at the lowest scattering angles.

Firstly, we have chosen to analyse the experimental correlation functions by the inverse Laplace transform technique, $C(q,t) = \int L(\ln\tau)\exp(-t/\tau)\mathrm{d}\ln\tau$, to obtain the distribution relaxation function $L(\ln\tau)$. The isotropic interdiffusion process is expectedly unimodal conforming to a single exponential function (eq. (15)) whereas the anisotropic $C_{vh}(q,t)$ clearly displays a bimodal $L(\ln\tau)$ (Fig. 3); the experimental $C_{vh}(q,t)$ can be also represented by a double exponential decay function. The amplitude of the slow process initially decreases with θ from 12° to 20° and then increases above 40° (see Fig. 6 below). While the origin of the initial reduction with scattering angle might be obscured by a possible contribution from the strong polarized intensity (strong at low q's, eq. (5)), the fact that the slow VH contribution increases with further increase of theta (Fig. 6) irrespectively of the laser wavelength (633 nm, 532 nm) excludes any spurious effects; under the same conditions, I_{vv} is by a factor of two weaker at 633 nm (eq. (3)). The variation of the shape of the anisotropic $C_{vh}(q,t)$ with scattering angle for PDMS/PEMS (A) (ξ = 27 nm at 313.8 K) and (B) (ξ = 54 nm at 322.4 K) is shown in Fig. 4 for theta 15, 30 and

Tab. 1. Molecular characteristics of the polymer blends: average degree of polymerization N, average statistical segment a, monomer volume v, average refraction index n and difference in refraction indices Δn, critical temperature T^* and parameters A, B and α (see Eq. (24))

Blend	N	a/Å	v/Å^3	A	B	α	n	Δn	T^* in °C
PS/PI	26.5	6.4	144	39	0.0419	1.55	1.54	0.11	95
PS/PB	20	5.9	126	37.9	0.0111	1.11	1.55	0.075	66
PDMS/PEMS A	252	5.3	149	3.22	0.0029	1.40	1.40	0.025	36
PDMS/PEMS B	249	5.3	149	3.22	0.0029	1.40	1.40	0.025	45.5
PDMS/PEMS C	275	5.3	149	3.22	0.0029	1.40	1.40	0.025	55

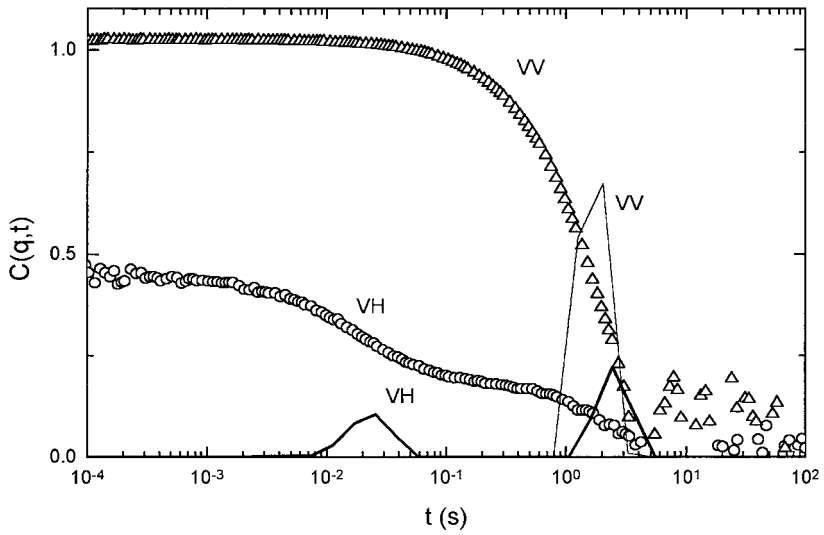

Fig. 3. Experimental anisotropic (VH) and isotropic (VV) scattering functions for PDMS/PEMS A at 313.8 K, θ =12° and $k\xi$ = 0.44 (λ = 532 nm) along with the corresponding distribution relaxation $L(\ln\tau)$ functions

70°. Up to about 55°, the experimental $C_{vh}(q, t)$ can be described by two distinct relaxation modes. From the two processes, the slow Γ_s relaxation rate clearly increases with theta, whereas the fast Γ_f rate exhibits a weaker variation with θ.

Based on this data analysis, the contribution of the slow process (second peak in $L(\ln\tau)$ of Fig. 3) was found to increase above about 40° whereas the intensity I_f of the fast process remains virtually constant. This can be hardly justified as VV leakage since the polarized I_{vv} intensity is a decreasing function of q (and hence θ). Moreover, the same behavior is also observed at T = 48.3°C for which I_{vv} is about three times weaker than at T = 40.7°C. We therefore claim that two relaxation processes are present in $I_{vh}(\mathbf{q}, t)$ from which the slow one dominates above $\theta \simeq 40°$; in fact, it is this slow process that was reported in ref.[3] For $\theta \gtrsim 55°$ the relaxation spectrum looks like one broad mode (rather than two modes) which becomes more narrow as θ is further increased. At θ = 150° the decay is almost single exponential with better than 2% accuracy (see Fig. 4f and the lower plot in Fig. 2).

Next we compare the experimental depolarized intensities with the theoretical predictions (eqs. (20), (B2), (10)). It is convenient to consider the scattering intensity normalized by the initial intensity, I_0, and the scattering volume, V_{eff}, taking into account the relative distance to the critical point $\Delta T/T^* = (T^* - T)/T^*$:

$$J \equiv \frac{I_{vh}(\Delta T/T^*)^2}{I_0 V_e ff} = k^8 n^4 \left(\frac{\Delta n}{2\pi}\right)^4 \left(\frac{Nv}{a}\right)^2 L_i \times 0.94 \qquad (24)$$

where a is the proportionality coefficient between τ, used in theory, and $\Delta T/T^*$ measured in experiment: τ =

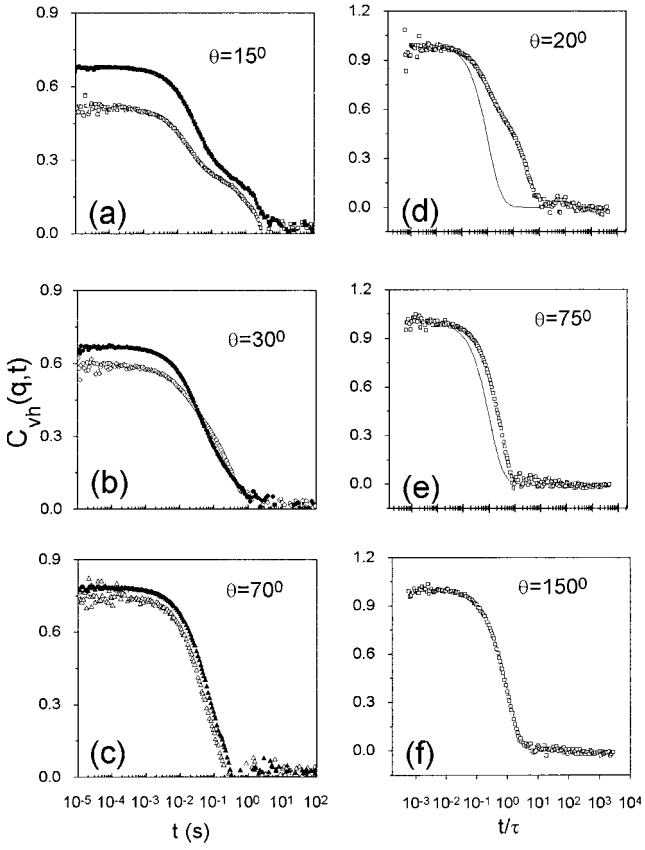

Fig. 4. Experimental anisotropic relaxation function (a)–(c) for PDMS/PEMS A ($k\xi$ = 0.44, T = 313.8 K) and B ($k\xi$ = 0.87, T = 322.4 K) shown respectively as open and solid symbols at three scattering angles. Theoretical predictions (d)–(f) are shown as solid curves together with experimental data for blend A

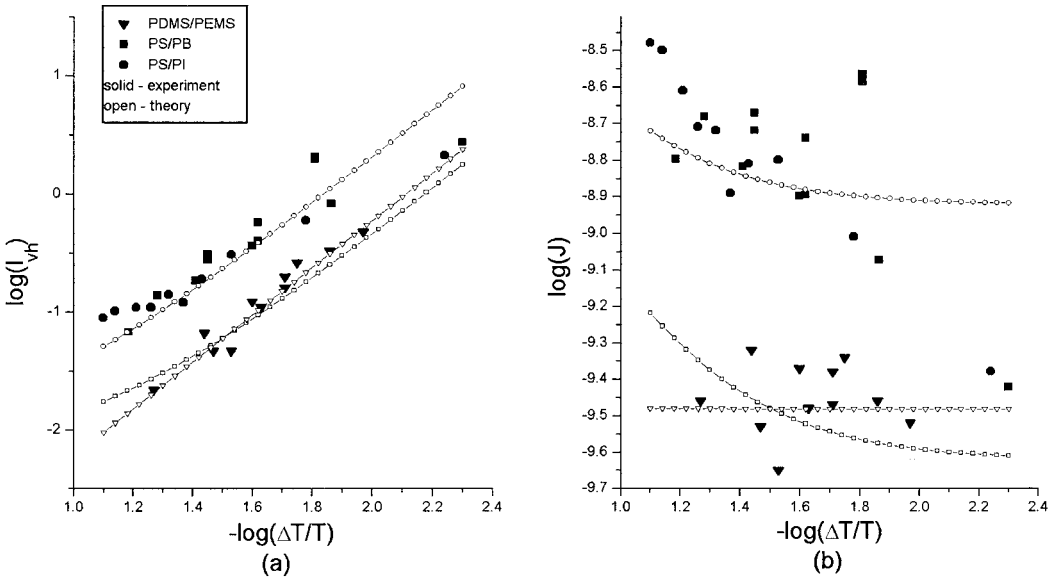

Fig. 5. Comparison between the experimental and theoretical (a) absolute values of the scattering intensities and (b) renormalized scattering intensities J defined by eq. (24)

$a\Delta T/T^*$, $\Delta n = n_1 - n_2$ is the difference of the refractive indices of two components. We use the standard approximation: $\chi(T) = A/T - B$ together with literature values for the parameters A and B. The definition of τ implies that $a = 1 + BN/2$. Numerical values of the relevant parameters used in calculations are listed in Table 1.

Computed (using the results obtained in section 5 and in Appendix B) and measured depolarized intensities at $\theta = 90^\circ$ for the three homogeneous blends at different temperatures near phase separation are plotted in Fig. 5. One can see a good agreement between the predictions and the experimental results for relatively long chain PDMS/PEMS blends as well as for short chain PS/PI blend, whereas for the PS/PB blend the calculated I_{vh} is about 5 times weaker than the experimental intensities. For the latter blend (PS/PB), the experimental slope of the log-log plot $I_{vh}(\Delta T/T)$ is smaller than 2. The deviation of the theoretical predictions for J from horizontal line means that the non-singular term is significant in the corresponding region. Note that for PS/PI and PS/PB blends, the non-singular term is noticeable (in comparison with the singular one) only far enough from the critical point (for $\Delta T/T > 0.03$, see left part of plots in Fig. 5). For PDMS/PEMS, the singular term dominates for all temperatures under consideration since the polymerization degree of PDMS/PEMS is about 10 times higher than for the other two blends.

The behavior of $I_{vh}(\theta)$ as a function of the scattering angle depends on temperature because of the temperature dependence of ξ. The theory (eq. (10)) predicts $I_{vh}(\theta) = const$ for small $k\xi$. For larger $k\xi$ a maximum of I_{vh} at $\theta \approx 75^\circ$ is predicted; the intensity decreases at higher angles (see Fig. 6). On the experimental side, $I_{vh}(\theta)$ normalized to that of the neat toluene also shows a maximum, which is more pronounced however than the theoretical prediction. Moreover, the experimental I_{vh} exhibits an additional increase at very high angles. This latter feature is not predicted. Nevertheless, the predicted maximum occurs in the vicinity of 75° irrespectively of k_0 and q as indicated by the data taken with $\lambda = 633$ nm. The I_{vh} for PDMS/PEMS (B) with larger $k\xi$ is indeed higher than the I_{vh} of (A) with lower $k\xi$. It is noticeable that the theoretical broad peak around $\theta = 75^\circ$ encompasses the two peak experimental pattern of $I_{vh}(\theta)$.

Let us compare now the observed relaxation rates and non-exponentiality parameters β or dynamic scattering processes with the theoretical predictions. The time dependencies have been fitted by the "stretched" exponential, $I(t) = I(0)\exp(-(\Gamma t)^\beta)$ for all angles higher than 40°. At lower angles $\theta \leq 40^\circ$ two relaxation processes were experimentally observed (Fig. 3, 4). Over the $\theta = 40 \div 150^\circ$, the predicted β for $k_0\xi = 0.4$ (Fig. 2b) agrees well with the values obtained from the experimental VH scattering functions. The non-exponentiality parameter β is close to 1 for large angles and is around 0.9 for small angles except for one point $\theta = 15^\circ$ both in theory and experiment (Fig. 2(b)). Note that the accuracy of fitting by two stretched exponents for such small angles ($\theta \leq 15^\circ$) is poor.

As shown in Fig. 7, Γ_{vh} is higher than $\Gamma_{vv} = 4Dk_0^2\sin^2\theta$ both in the theory and in the experiment. The experimental fast rates expressed as reduced quantities $\Gamma_{vh}/(4Dk_0^2)$ compare well with the theoretical reduced rates, which vary from about 0.6 to 1, respectively, at low and high angles for $k\xi = 1$. In fact, PDMS/PEMS A and B mimic the theoretical behavior for low and high $k\xi$, respectively;

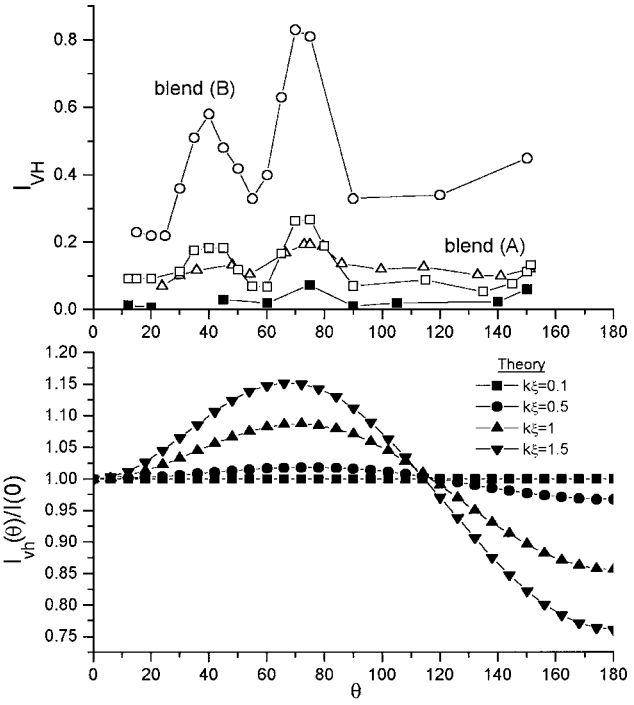

Fig. 6. The experimental (upper) and theoretical (lower) angular dependencies of the depolarized intensities. Theoretical curves are shown for four different $k_0\xi$ values. The experimental intensities are for two PDMS/PEMS blends: for A at T = 313.8 K and λ = 532 nm ($k\xi$ = 0.44) and 633 nm ($k\xi$ = 0.39) shown as open squares and triangles, respectively; at T = 321 K, λ = 532 nm ($k\xi$ = 0.21) as solid squares. The data for the blend B are shown by open cycles at T = 322.4 K, λ = 532 nm ($k\xi$ = 0.87)

with increasing $k\xi$, $\Gamma_{vh}/(4Dk_0^2)$ decreases at low angles. The experimental relaxation rate also tends to 1 for large angles, but for small angles it is more close to Γ_{vv}. This feature can be explained in part by the fact that most Γ_{vh} shown in Fig. 7 had been obtained from the experimental correlation function after extraction of fast VH mode which gains intensity at low angles.

Finally, a more direct comparison between theoretical and experimental scattering functions for PDMS/PEMS A is shown in Fig. 4. Note two relaxation processes observed for θ = 20°. The fast process disappears at higher scattering angles, so that the data and the theory are in agreement for higher angles, the agreement being very good for θ = 150°.

7. Conclusion

In conclusion, we presented a theoretical interpretation of the depolarized light scattering of polymer blends in terms of the double scattering process. The theory accounts for many observed features of the depolarized scattering. In particular, note a good agreement between the predicted and the measured temperature dependencies of the depolarized intensity for PDMS/PEMS blends

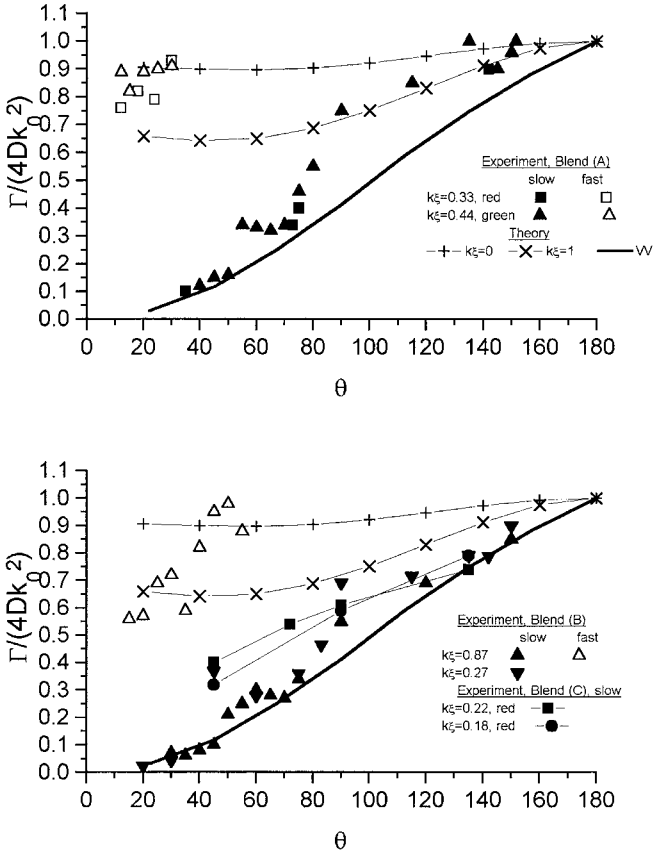

Fig. 7. Comparison between theoretical and experimental relaxation rates for the anisotropic scattering from PDMS/PEMS mixtures as a function of the scattering angle. Solid (thick) line denotes the variation of the interdiffusion rate $4Dk_0^2 \sin^2(\theta/2)$, whereas the thinner solid lines with (+) and (×) are the theoretical predictions for $\Gamma_{vh}/(4Dk_0^2)$ for two different $k_0\xi$ values. The empty symbols denote the experimental reduced fast rate whereas the solid symbols are for the experimental reduced slow rate in three PDMS/PEMS blends: A at T = 313.8 K, λ = 532 nm (triangle) and λ = 633 nm (squares), B at T = 322.4 K and λ = 532 nm (cycles); and C at T = 338 K at λ = 488 nm (ref. [3])

which was obtained with no adjustable parameters: it is the absolute intensities (rather than reduced ones) that are compared.

However several observations have not been explained by the theory:

1. The measured intensity for PS/PB blend is much higher than the predicted one. Note that the predicted intensity is quite sensitive to the position of the critical point which might not be known accurately enough.
2. A noticeable fast mode is observed for PDMS/PEMS blends at low scattering angles. It is tempting to attribute this fast mode to the initial (short time) VH relaxation, which is predicted to relax with the reduced rate $\Gamma_{vh}^0/(4Dk_0^2) \approx 1$ (see section 4), and the slow mode to the long-time relaxation tail with $\Gamma_{vh}^\infty/(4Dk_0^2) = 1 - \cos\frac{\theta}{2}$. However the theoretical ratio of intensities of these modes I_{fast}/I_{slow} is much lower than that obtained experimentally.

It might be also tempting to attribute the fast mode to the non-singular contribution to dynamic double scattering which is also characterized by fast decay. An analysis shows, however, that the non-singular intensity is too low in comparison with that observed. An interesting feature of the fast mode is that its relaxation rate is increasing as the scattering angle decreases: this is an unusual behavior.

3. The observed VH intensity sharply increases at very high angles while the theory predicts a (smooth) decrease of I_{vh} in this regime. We are leaving elucidation of the above points for future efforts.

Appendix A: Derivation of a general expression for double scattering

In this appendix we present the derivation of eq. (9) for the depolarized scattering intensity for arbitrary structure factor and form factor of the sample. We start from eq. (8) and substitute the amplitude of the single scattered wave $E^{(1)}$ from equation (7):

$$\mathbf{E}_{vh}(\mathbf{R}) = -k_0^2 \frac{e^{ik_0R_0}}{R_0} E_0 \int (\mathbf{e}_0\mathbf{q})(\mathbf{q}\mathbf{e}_1)\, æ(\mathbf{q}')\, æ(\mathbf{q}-\mathbf{k}_0)$$

$$\cdot \frac{e^{i(\mathbf{q}\mathbf{r}_1+\mathbf{q}'\mathbf{r}-\mathbf{k}\mathbf{r}+k_0|\mathbf{r}-\mathbf{r}_1|)}}{|\mathbf{r}-\mathbf{r}_1|} H(\mathbf{r})H(\mathbf{r}_1)d^3r d^3r_1 \frac{d^3q}{(2\pi)^3}\frac{d^3q'}{(2\pi)^3}$$

Then we change variables as $\mathbf{r}_1 \to \mathbf{r}_2 = \mathbf{r}_1 - \mathbf{r}$ and introduce the Fourier image of the form factor $H(\mathbf{q}) = \int H(\mathbf{r}) e^{i\mathbf{q}\mathbf{r}} d^3r$, $H(\mathbf{r}) = \int H(\mathbf{q}_1) e^{-i\mathbf{q}_1\mathbf{r}} \frac{d^3\mathbf{q}_1}{(2\pi)^3}$,

$$\mathbf{E}_{vh}(\mathbf{R}) = -k_0^2 \frac{e^{ik_0R_0}}{R_0} E_0 \int (\mathbf{e}_0\mathbf{q})(\mathbf{q}\mathbf{e}_1)\, æ(\mathbf{q}')\, æ(\mathbf{q}-\mathbf{k}_0)$$

$$\cdot \frac{e^{i(\mathbf{q}\mathbf{r}_2+k_0r_2-\mathbf{q}_2\mathbf{r}_2)}}{r_2} e^{i(\mathbf{q}+\mathbf{q}'-\mathbf{k}-\mathbf{q}_1-\mathbf{q}_2)} H(\mathbf{q}_1)H(\mathbf{q}_2)$$

$$\cdot \frac{d^3q}{(2\pi)^3}\frac{d^3q_1}{(2\pi)^3}\frac{d^3q'}{(2\pi)^3}\frac{d^3q_2}{(2\pi)^3} d^3r d^3r_2$$

Then we can take the integral over $\mathbf{r}$, which gives $\delta(\mathbf{q}_2 - (\mathbf{q} + \mathbf{q}' - \mathbf{k} - \mathbf{q}_1))$ and then integrate over $\mathbf{q}_2$:

$$\mathbf{E}_{vh}(\mathbf{R}) = -\left(\frac{w}{c}\right)^2 \frac{e^{i\frac{w}{c}\mathbf{R}_0}}{R_0} E_0 \int (\mathbf{e}_0\mathbf{q})(\mathbf{q}\mathbf{e}_1)\, æ(\mathbf{q}')\, æ(\mathbf{q}-\mathbf{k}_0)$$

$$\cdot \frac{e^{i(\mathbf{r}_2(\mathbf{k}-\mathbf{q}'+\mathbf{q}_1)+k_0r_2)}}{r_2} H(\mathbf{q}_1)H(\mathbf{q}+\mathbf{q}'-\mathbf{k}-\mathbf{q}_1)$$

$$\cdot \frac{d^3q}{(2\pi)^3}\frac{d^3q_1}{(2\pi)^3}\frac{d^3q'}{(2\pi)^3} d^3r_2$$

Let us introduce a function $f(\mathbf{q}) = (\mathbf{e}_0\mathbf{q})(\mathbf{e}_1\mathbf{q}) \int \frac{e^{i(\mathbf{q}\mathbf{r}+kr)}}{r} d^3r$ and make use of the fact that the function $H(\mathbf{q})$ is localized in the region $q < \frac{1}{L} \ll k$, so that $q_1 \ll k$ and $\mathbf{q} \approx \mathbf{k} - \mathbf{q}'$:

$$\mathbf{E}_{vh}(\mathbf{R}) = -\left(\frac{w}{c}\right)^2 \frac{e^{i\frac{w}{c}\mathbf{R}_0}}{R_0} E_0 \int æ(\mathbf{q}')\, æ(\mathbf{q}-\mathbf{k}_0) f(\mathbf{k}-\mathbf{q}'+\mathbf{q}_1)$$

$$\cdot H(\mathbf{q}_1)H(\mathbf{q}+\mathbf{q}'-\mathbf{k}-\mathbf{q}_1)\frac{d^3q}{(2\pi)^3}\frac{d^3q'}{(2\pi)^3}\frac{d^3q_1}{(2\pi)^3}$$

$$I_{vh} = \frac{c}{4\pi}\left(\frac{w}{c}\right)^4 E_0^2 \int f(\mathbf{k}-\mathbf{q}'+\mathbf{q}_1) f(\mathbf{k}-\mathbf{Q}'+\mathbf{Q}_1)$$

$$\cdot \langle æ(\mathbf{q}')\, æ(\mathbf{q}-k_0)\, æ(-\mathbf{Q}')\, æ(\mathbf{k}_0-\mathbf{Q})\rangle$$

$$\cdot H(\mathbf{q}_1)H(\mathbf{Q}_1)H(\mathbf{q}+\mathbf{q}'-\mathbf{k}-\mathbf{q}_1)H(\mathbf{Q}+\mathbf{Q}'-\mathbf{k}-\mathbf{Q}_1)$$

$$\cdot \frac{d^3q}{(2\pi)^3}\frac{d^3q_1}{(2\pi)^3}\frac{d^3q'}{(2\pi)^3}\frac{d^3Q}{(2\pi)^3}\frac{d^3Q'}{(2\pi)^3}\frac{d^3Q_1}{(2\pi)^3}$$

At this stage we use the Wick's theorem valid for Gaussian fluctuations[12]:

$$\langle æ(\mathbf{q}_1)\, æ(\mathbf{q}_2)\, æ(\mathbf{q}_3)\, æ(\mathbf{q}_4)\rangle = \langle æ(\mathbf{q}_1)\, æ(\mathbf{q}_2)\rangle$$

$$\cdot \langle æ(\mathbf{q}_3)\, æ(\mathbf{q}_4)\rangle + \langle æ(\mathbf{q}_1)\, æ(q_3)\rangle\langle æ(\mathbf{q}_2)\, æ(\mathbf{q}_4)\rangle$$

$$+ \langle æ(\mathbf{q}_1)\, æ(\mathbf{q}_4)\rangle\langle æ(\mathbf{q}_2)\, æ(\mathbf{q}_3)\rangle$$

Using the definition of the structure factor $\langle \delta\phi(\mathbf{q}_1)\delta\phi(\mathbf{q}_2)\rangle = (2\pi)^3 S(\mathbf{q}_1)\delta(\mathbf{q}_1 + \mathbf{q}_2)$ we get

$$\langle æ\mathbf{q}')\, æ(\mathbf{q}-\mathbf{k}_0)\, æ(-\mathbf{Q}')\, æ(\mathbf{k}_0-\mathbf{Q})\rangle =$$

$$\left(\frac{A}{2\pi}\right)^4 S(\mathbf{q}')S(\mathbf{q}-\mathbf{k}_0)(2\pi)^6(\delta(\mathbf{q}'-\mathbf{Q}')\delta(\mathbf{q}-\mathbf{Q})$$

$$+\delta(\mathbf{q}'-\mathbf{Q}+\mathbf{k}_0)\delta(-\mathbf{Q}'+\mathbf{q}-\mathbf{k}_0))$$

where $\frac{A}{2\pi}$ is a proportionality coefficient between $æ(\mathbf{q})$ and $\delta\phi(\mathbf{q})$. Note that the third term will contain after integration the term $H(\mathbf{k} - \mathbf{k}_0)$ which is non-negligible only for $|\mathbf{k} - \mathbf{k}_0| \ll k_0$, i.e. it can be neglected provided that the scattering angle is not extremely small. Thus

$$I_{vh} = \frac{c}{4\pi}\left(\frac{w}{c}\right)^4 E_0^2 \int S(\mathbf{q}')S(\mathbf{q}-\mathbf{k}_0) f(\mathbf{k}-\mathbf{q}'+\mathbf{q}_1)$$

$$\cdot H(\mathbf{q}_1)H(\mathbf{Q}_1)H(\mathbf{q}+\mathbf{q}'-\mathbf{k}-\mathbf{q}_1)H(\mathbf{q}+\mathbf{q}'-\mathbf{k}-\mathbf{Q}_1)$$

$$\cdot (f^*(\mathbf{k}-\mathbf{q}+\mathbf{Q}_1) + f^*(\mathbf{k}+\mathbf{k}_0-\mathbf{q}+\mathbf{Q}_1))$$

$$\cdot \frac{d^3q}{(2\pi)^3}\frac{d^3q'}{(2\pi)^3}\frac{d^3Q_1}{(2\pi)^3}\frac{d^3q_1}{(2\pi)^3}$$

Then we do a number of substitutions and obtain the final result, taking into account that the argument of $H(\mathbf{q})$ is always smaller than k_0 and that

$$\int H(\mathbf{q})H(\mathbf{q}+\mathbf{q}_1)\frac{\mathrm{d}^3q}{(2\pi)^3} =$$

$$\int H(\mathbf{r}_1)H(\mathbf{r}_2)\mathrm{e}^{\mathrm{i}(\mathbf{r}_1\mathbf{q}+\mathbf{r}_2(\mathbf{q}+\mathbf{q}_1))}\frac{\mathrm{d}^3q}{(2\pi)^3}\mathrm{d}^3r_1\mathrm{d}^3r_2 =$$

$$\int H^2(\mathbf{r}_1)^{\mathrm{i}\mathbf{r}_1\mathbf{q}_1}\mathrm{d}^3r_1 = H(\mathbf{q}_1) \qquad (A1)$$

since $H^2(\mathbf{r}) = H(\mathbf{r})$ by definition.

1) $\mathbf{q}' \rightarrow \mathbf{q}'' = \mathbf{q}' - \mathbf{k} + \mathbf{q}$:

$$I_{vh} = \frac{c}{4\pi}\left(\frac{w}{c}\right)^4 E_0^2 \int S(\mathbf{q}''+\mathbf{k}-\mathbf{q})S(\mathbf{q}-\mathbf{k}_0)f(\mathbf{q}-\mathbf{q}''+\mathbf{q}_1)$$

$$\cdot H(\mathbf{q}_1)H(\mathbf{Q}_1)H(\mathbf{q}''-\mathbf{q}_1)H(\mathbf{q}''-\mathbf{Q}_1)(f^*(\mathbf{q}-\mathbf{q}''+\mathbf{Q}_1)$$

$$+f^*(\mathbf{k}+\mathbf{k}_0-\mathbf{q}+\mathbf{Q}_1))\frac{\mathrm{d}^3q}{(2\pi)^3}\frac{\mathrm{d}^3q''}{(2\pi)^3}\frac{\mathrm{d}^3Q_1}{(2\pi)^3}\frac{\mathrm{d}^3q_1}{(2\pi)^3}$$

Whence we conclude that $q_1 \ll k_0$, $Q_1 \ll k_0$, $q'' \ll k_0$.

2) $\mathbf{q} \rightarrow \mathbf{q}_n = \mathbf{q} + \mathbf{q}_1 - \mathbf{q}''$. Here we can neglect $\mathbf{q}_1$ and $\mathbf{q}''$ in S:

$$I_{vh} = \frac{c}{4\pi}\left(\frac{w}{c}\right)^4 E_0^2 \int S(\mathbf{k}-\mathbf{q}_n)S(\mathbf{q}_n-\mathbf{k}_0)f(\mathbf{q}_n)H(\mathbf{q}_1)$$

$$\cdot H(\mathbf{Q}_1)H(\mathbf{q}''-\mathbf{q}_1)H(\mathbf{q}''-\mathbf{Q}_1)(f^*(\mathbf{q}_n-\mathbf{q}_1+\mathbf{Q}_1)$$

$$+f^*(\mathbf{k}+\mathbf{k}_0-\mathbf{q}_n-\mathbf{q}''+\mathbf{q}_1+\mathbf{Q}_1))$$

$$\cdot\frac{\mathrm{d}^3q_n}{(2\pi)^3}\frac{\mathrm{d}^3q''}{(2\pi)^3}\frac{\mathrm{d}^3Q_1}{(2\pi)^3}\frac{\mathrm{d}^3q_1}{(2\pi)^3}$$

3) This step must be done separately for two terms containing f^*:

a) $\mathbf{Q}_1 \rightarrow \mathbf{Q}_2 = \mathbf{Q}_1 - \mathbf{q}_1$:

$$I_{vh}^{(a)} = \frac{c}{4\pi}\left(\frac{w}{c}\right)^4 E_0^2 \int S(\mathbf{k}-\mathbf{q}_n)S(\mathbf{q}_n-\mathbf{k}_0)f(\mathbf{q}_n)H(\mathbf{q}_1)$$

$$\cdot H(\mathbf{Q}_2+\mathbf{q}_1)H(\mathbf{q}''-\mathbf{q}_1)(f^*(\mathbf{q}_n-\mathbf{Q}_2)H(\mathbf{q}''-\mathbf{Q}_2-\mathbf{q}_1))$$

$$\cdot\frac{\mathrm{d}^3q_n}{(2\pi)^3}\frac{\mathrm{d}^3q''}{(2\pi)^3}\frac{\mathrm{d}^3Q_2}{(2\pi)^3}\frac{\mathrm{d}^3q_1}{(2\pi)^3}$$

Using eq. (A1) we get $\int H(\mathbf{q}''-\mathbf{q}_1)H(\mathbf{q}''-\mathbf{Q}_2-\mathbf{q}_1)\frac{\mathrm{d}^3q''}{(2\pi)^3} = H(\mathbf{Q}_2)$; $\int H(\mathbf{q}_1)H(\mathbf{Q}_2+\mathbf{q}_1)\frac{\mathrm{d}^3q_1}{(2\pi)^3} = H(\mathbf{Q}_2)$ and obtain

$$I_{vh}^{(a)} = \frac{c}{4\pi}\left(\frac{w}{c}\right)^4 E_0^2 \int S(\mathbf{k}-\mathbf{q}_n)S(\mathbf{q}_n-\mathbf{k}_0)f(\mathbf{q}_n)$$

$$\cdot f^*(\mathbf{q}_n-\mathbf{Q}_2)H^2(\mathbf{Q}_2)\frac{\mathrm{d}^3q_n}{(2\pi)^3}\frac{\mathrm{d}^3Q_2}{(2\pi)^3}$$

b) $\mathbf{Q}_1 \rightarrow \mathbf{Q}_2 = \mathbf{Q}_1 + \mathbf{q}_1 - \mathbf{q}''$:

$$I_{vh}^{(b)} = \frac{c}{4\pi}\left(\frac{w}{c}\right)^4 E_0^2 \int S(\mathbf{k}-\mathbf{q}_n)S(\mathbf{q}_n-\mathbf{k}_0)f(\mathbf{q}_n)H(\mathbf{q}_1)$$

$$\cdot H(\mathbf{Q}_2-\mathbf{q}_1+\mathbf{q}'')H(\mathbf{q}''-\mathbf{q}_1)f^*(\mathbf{k}+\mathbf{k}_0-\mathbf{q}_n+\mathbf{Q}_2)$$

$$\cdot H(-\mathbf{Q}_2+\mathbf{q}_1)\frac{\mathrm{d}^3q_n}{(2\pi)^3}\frac{\mathrm{d}^3q''}{(2\pi)^3}\frac{\mathrm{d}^3Q_2}{(2\pi)^3}\frac{\mathrm{d}^3q_1}{(2\pi)^3}$$

Using eq. (A1) $\int H(\mathbf{q}''-\mathbf{q}_1)H(\mathbf{Q}_2-\mathbf{q}_1+\mathbf{q}'')\frac{\mathrm{d}^3q''}{(2\pi)^3} = H(\mathbf{Q}_2)$; $\int H(\mathbf{q}_1)H(\mathbf{q}_1-\mathbf{Q}_2)\frac{\mathrm{d}^3q_1}{(2\pi)^3} = H(\mathbf{Q}_2)$. Thus we get total intensity $I_{vh} = I_{vh}^{(a)} + I_{vh}^{(b)}$:

$$I_{vh} = \frac{c}{4\pi}\left(\frac{w}{c}\right)^4 E_0^2 \int S(\mathbf{k}-\mathbf{q})S(\mathbf{q}-\mathbf{k}_0)f(\mathbf{q})H^2(\mathbf{Q}_2)$$

$$\cdot(f^*(\mathbf{q}-\mathbf{Q}_2)+f^*(\mathbf{k}+\mathbf{k}_0-\mathbf{q}+\mathbf{Q}_2))\frac{\mathrm{d}^3Q_2}{(2\pi)^3}\frac{\mathrm{d}^3q}{(2\pi)^3}$$

Substituting $\mathbf{q}$ for $\mathbf{q} - \mathbf{Q}_2$ we finally obtain eq. (9).

Appendix B: Generalization for the case $n \neq 1$

In sections 2–5 we assumed that the mean refractive index of the blend is close to unity $n \approx 1$. Here we generalize the results, equations (20), (23), for any n. This will allow us to compare the absolute values of the intensities.

In the general case starting from Maxwell's equations we get the following equation describing a single scattering event[4)]

$$\mathrm{rot\ rot}\ \mathbf{E} = \mathrm{grad\ div}\ \mathbf{E} - \Delta\mathbf{E} = -\frac{\epsilon}{c^2}\frac{\partial^2\mathbf{E}}{\partial t^2}$$

where $\epsilon = n^2$ is the polymer dielectric constant, $\mathbf{E} = \mathbf{E}^{(0)} + \mathbf{E}'$ is the sum of the initial and the scattered waves. After some simplifications we obtain an equation for the single scattered wave

$$\frac{\epsilon}{c^2}\frac{\partial^2\mathbf{E}'}{\partial t^2} - \Delta\mathbf{E}' = 4\pi\ \mathrm{grad}\frac{1}{n^2}\mathrm{div}\,æ\mathbf{E}^{(0)} \qquad (B1)$$

The solution of this equation has the same form as the first term in equation (7) with additional prefactor n^{-2} and $k = n(w/c)$. The prefactor leads to an additional factor of n^{-8} in the double scattered intensity (since we apply equation (B1) twice, and then raise the amplitude to the second power) and the second point leads to the factor n^8 in singular term for the double scattering intensity (since it is proportional to k^8) and to the factor n^4 in non-singular term. Hence the two points cancel each other in singular contribution and the non-singular contribution stays with the additional factor n^{-4}.

We also have to use a more accurate relation between $\frac{\partial æ}{\partial\phi}$ and A: $\frac{\partial æ}{\partial\phi} = \frac{n}{2\pi}A$ (compare with eq. (2)); this renor-

malization gives rise to the additional factor n^4 in the VH intensity.

Thus we obtain the following renormalization of eq. (20):

$$I^s_{vh} \to n^4 I^s_{vh} \tag{B2}$$

while the non-singular term remains the same due to cancellation of the two factors.

Acknowledgement: Part of this research was sponsored by *NATO's Scientific Affairs Division* in the framework of the Science for Stability Programme. A.E.L. also acknowledges partial support by the *Royal Society/NATO Postdoctoral Fellowship Programme.*

[1] P. G. DeGennes, *"Scaling Concepts in Polymer Physics"*, Cornell Univ. Press, Ithaca, NY 1985
[2] K. Binder, *Adv. Polym. Sci.* **112**, 181 (1994)
[3] G. Fytas, D. Vlassopoulos, G. Meier, A. E. Likhtman, A. N. Semenov, *Phys. Rev. Lett.* **76**, 3586 (1996)
[4] L. D. Landau, E. M. Lifshitz, *"Electrodynamics of continuous media"*, Pergamon, Oxford 1960
[5] B. Berne, R. Pecora, *"Dynamic Light Scattering"*, J. Wiley, N. Y. 1976
[6] J. Higgins, H. Benoit, *"Polymers and neutron scattering"*, Oxford University Press, 1994
[7] G. Fytas, G. Meier, in *"Dynamic Light Scattering"*, ch. 10, W. Brown, Ed., Clarendon Oxford, 1993
[8] M. J. Stephen, *Phys. Rev.* **187**, 279 (1969); C. M. Sorensen, R. C. Mockler, J. O. Sullivan, *Phys. Rev. A* **14**, 1520 (1976); J. P. Mc Tague, G. Birnbaum, *Phys. Rev. Lett.* **21**, 661 (1968); P. Madden, *Mol. Phys.* **36**, 365 (1978); G. Li, W. M. Du, X. K. Chen, H. Z. Cummins, N. J. Tao, *Phys. Rev. A* **45**, 3867 (1992)
[9] T. Jian, A. N. Semenov, S. H. Anastasiadis, G. Fytas, *J. Chem. Phys.* **100**, 3286 (1994)
[10] A. N. Semenov, A. R. Khokhlov, *Usp. Fiz. Nauk* **156**, 427 (1988)
[11] L. D. Landau, E. M. Lifshitz, *"Statistical Physics"*, Pergamon Press, Oxford 1998
[12] L. D. Landau, E. M. Lifshitz, *"Statistical Physics"*, Part 2, Butterworth-Heinemann, 1995